Published in final edited form as:
Neuropharmacology. 2011 ; 60(2-3): 520–528. doi:10.1016/j.neuropharm.2010.11.009.

Allosteric modulators induce distinct movements at the GABA-binding site interface of the GABA-A receptor

Feyza Sancar[1] and **Cynthia Czajkowski**[*]
Department of Physiology, University of Wisconsin-Madison, Madison, Wisconsin

Abstract

Benzodiazepines (BZDs) and barbiturates exert their CNS actions by binding to GABA-A receptors (GABARs). The structural mechanisms by which these drugs allosterically modulate GABAR function, to either enhance or inhibit GABA-gated current, are poorly understood. Here, we used the substituted cysteine accessibility method to examine and compare structural movements in the GABA-binding site interface triggered by a BZD positive (flurazepam), zero (flumazenil) and negative (3-carbomethoxy-4-ethyl-6, 7-dimethoxy-β-carboline, DMCM) modulator as well as the barbiturate pentobarbital. Ten residues located throughout the GABA binding site interface were individually mutated to cysteine. Wild-type and mutant $\alpha_1\beta_2\gamma_2$ GABARs were expressed in *Xenopus laevis* oocytes and functionally characterized using two-electrode voltage clamp. We measured and compared the rates of modification of the introduced cysteines by sulfhydryl-reactive methanethiosulfonate (MTS) reagents in the absence and presence of BZD-site ligands and pentobarbital. Flurazepam and DMCM each accelerated the rate of reaction at α_1R131C and slowed the rate of reaction at α_1E122C, whereas flumazenil had no effect indicating that simple occupation of the BZD binding site is not sufficient to cause movements near these positions. Therefore, BZD-induced movements at these residues are likely associated with the ability of the BZD to modulate GABAR function (BZD efficacy). Low, modulating concentrations of pentobarbital accelerated the rate of reaction at α_1S68C and β_2P206C, slowed the rate of reaction at α_1E122C and had no effect at α_1R131C. These findings indicate that pentobarbital and BZDs induce different movements in the receptor, providing evidence that the structural mechanisms underlying their allosteric modulation of GABAR function are distinct.

Keywords

$GABA_A$ receptor; benzodiazepine efficacy; oocyte expression; allosteric modulation; pentobarbital; GABA

1. Introduction

$GABA_A$ receptors (GABARs), besides being activated by the neurotransmitter GABA, are modulated by numerous therapeutically important drugs, including barbiturates, anesthetics, and benzodiazepines (BZDs). These compounds are allosteric modulators as they bind to

[*]Corresponding author. Tel.:(608) 265-5863; Fax: (608) 265-5512; czajkowski@physiology.wisc.edu; mailing address: Department of Physiology, University of Wisconsin-Madison, 601 Science Drive, Madison, WI 53711.
[1]Current affiliation: Department of Biological Sciences, University of Illinois-Chicago, 840 W. Taylor Street, MC067, Chicago, IL

sites distinct from the orthosteric GABA binding sites to potentiate or inhibit GABA-evoked current. Significant strides have been made in identifying the binding sites for these modulators (see (Hemmings et al., 2005; Mitchell et al., 2008; Sigel, 2002) for reviews). However, the structural mechanisms that couple the binding of these modulators to the allosteric modulation of GABA-gated current are less well understood.

BZDs have varying effects on GABAR function. BZD-site agonists (e.g. diazepam and flurazepam), act as positive modulators to enhance GABA-gated current (I_{GABA}). BZD-site inverse agonists (e.g. DMCM) act as negative modulators to inhibit I_{GABA}, while BZD-site antagonists (e.g. flumazenil) bind but have no effect on I_{GABA} and thus act as "zero" modulators. The BZD binding site is located in the extracellular amino terminal domain, at the interface between the GABAR α and γ subunits (Pritchett et al., 1989; Smith and Olsen, 1995). Previous studies have identified residues in Loop F/9, the M2-M3 extracellular loop and the pre-M1 region of the γ2 subunit that are required for enhancement of I_{GABA} by BZD positive modulators (Boileau and Czajkowski, 1999; Boileau et al., 1998; Hanson and Czajkowski, 2008; Jones-Davis et al., 2005; Padgett and Lummis, 2008). Interestingly, these γ2 subunit residues/regions are not critical for inhibition of I_{GABA} by the BZD-site negative modulator, DMCM (Boileau and Czajkowski, 1999; Hanson and Czajkowski, 2008), suggesting that the structural pathways mediating BZD negative allosteric modulation are distinct from those involved in positive modulation.

Depending on the electrophysiological approach and kinetic models used, investigators have asserted that BZDs exert their allosteric effects on I_{GABA} by either altering the microscopic binding of GABA at the orthosteric site (Goldschen-Ohm et al., 2010; Lavoie and Twyman, 1996; Mellor and Randall, 1997; Rogers et al., 1994; Thompson et al., 1999; Twyman et al., 1989), or by shifting the closed to open state channel equilibrium of the agonist-bound receptor (Campo-Soria et al., 2006; Downing et al., 2005; Rusch and Forman, 2005). Regardless of the mechanism, because GABA binding and channel gating are energetically coupled (i.e. the open channel state of the GABAR has a higher affinity for GABA than the closed state), one would predict that BZD actions would result in structural rearrangements of the GABA binding site. Recently, we demonstrated that the GABA binding site undergoes structural rearrangement upon binding the positive BZD modulator flurazepam (Kloda and Czajkowski, 2007).

Here, we tested whether positive, negative, and zero allosteric modulators trigger distinct conformational movements within the GABA-binding site interface that are correlated with their efficacy. We mutated ten residues throughout the GABA binding site interface to cysteine (Fig. 1). We then measured the rate at which the introduced cysteines were modified by sulfhydryl-specific reagents in the absence and presence of flurazepam (BZD positive modulator), DMCM (BZD negative modulator), and flumazenil (BZD zero modulator) to probe the dynamics of the GABA binding interface upon binding BZD modulators that elicit different pharmacological effects. We also examined whether low concentrations of the positive allosteric modulator, pentobarbital, which binds at a site distinct from both the BZD and GABA binding sites (Amin, 1999;Belelli et al., 1999;Serafini et al., 2000), induces similar structural rearrangements at the GABA binding site interface as a BZD positive modulator.

2. Materials and Methods

2.1. Site directed mutagenesis

Rat cDNAs encoding for the GABAR α_1, β_2 and γ_2 subunits were used in this study. α_1 and β_2 cysteine mutants were engineered using the Altered Sites II in vitro Mutagenesis Systems (Promega Corp., Madison, WI) or by recombinant PCR, as described previously (Boileau et

al., 1999; Kucken et al., 2000). Cysteine substitutions were made in the rat α_1 subunit at positions T60, S68, E122, R131 and the rat β_2 subunit at positions L99, T160, G203, P206, R207 and S209 (Fig. 1) (Boileau et al., 1999; Boileau et al., 2002; Holden and Czajkowski, 2002; Kloda and Czajkowski, 2007; Newell et al., 2004; Wagner and Czajkowski, 2001). The α_1 and β_2 cysteine mutants were subcloned into pGH19 (Liman et al., 1992; Robertson et al., 1996) for expression in *Xenopus laevis* oocytes. All mutants were verified by restriction digest and double-stranded cDNA sequencing. All α_1 and $\beta_2$cy steine mutants have been named, using the single letter code, as wild-type residue, residue number (in the mature subunit protein), and mutated residue.

2.2. Expression in oocytes

Xenopus laevis oocytes were prepared, and then injected with cRNA as described previously (Boileau et al., 1998). In brief, cRNA encoding for the wild-type (WT) and mutant subunits were synthesized by *in vitro* transcription from NheI linearized cDNA template using the mMessage mMachine T7 kit (Ambion, Austin, TX). Oocytes were prepared by incubation in a collagenase solution (2mg/ml in ND96/Ca^{2+}-free media containing 96mM NaCl, 2mM KCl, 1mM $MgCl_2$ and 5mM HEPES, pH7.6), followed by several washes in recording solution. Within 1–2 days, WT or mutant α_1 and WT or mutant β_2 subunits were expressed with WT γ_2 subunits by injecting 25nl of αβγ cRNA mix into oocytes (at 5–25ng/ml cRNA for α_1 and β_2, and 50–250ng/μl cRNA for γ_2 to achieve a final ratio of 1:1:10/$\alpha_1\beta_2\gamma_2$). Oocytes were stored at 17–19 °C in recording solution (ND96 with 1.8mM $CaCl_2$; ND96/Ca^{2+}) Supplemented with 100μg/ml gentamicin and 100μg/ml bovine serum albumin for 2–14 days and used for electrophysiological recordings.

2.3. Voltage Clamp analysis

Oocytes were held at −80mV under two-electrode voltage clamp while continuously perfused with ND96/Ca^{2+} at a rate of 5ml/min in a bath volume of 200μl. Stock solutions of Flurazepam (RBI, Natick, MA), pentobarbital (Sigma, St. Louis, MO), and GABA (Sigma, St. Louis, MO) were dissolved in ND96/Ca^{2+}. Stock solutions of DMCM (RBI, Natick, MA), flumazenil (RBI, Natick, MA), N-biotinylaminoethyl methanethiosulfonate (MTSEA-biotin) and 2-sulfonatoethyl methanethiosulfonate (MTSES) (Toronto Research Chemicals, Toronto, Ontario, Canada) were prepared in DMSO and subsequently diluted in ND96/Ca^{2+} for working concentrations where the final [DMSO] (≤ 2%) did not affect GABAR function. Borosilicate electrodes (Warner Instruments, Hamden, CT) were filled with 3M KCl and had resistances between 0.5 and 2MΩ. Electrophysiological data were acquired with a GeneClamp 500 (Molecular Devices, Sunnyvale, CA) interfaced to a computer with a Digidata®1200 analog-to-digital device (Axon Instruments/Molecular Devices, Sunnyvale, CA) and recorded using the WinWCP Strathclyde Whole Cell Program, version 3.5.5 (kindly provided by J. Dempster, University of Strathclyde, Glasgow, UK).

GABA EC_{50} values for mutant and wild-type GABARs were previously established (Boileau et al., 1999; Boileau et al., 2002; Holden and Czajkowski, 2002; Kloda and Czajkowski, 2007; Newell et al., 2004; Wagner and Czajkowski, 2001). As such, for each mutant receptor, GABA EC_{50} was estimated by examining the ratio of response to a low concentration of GABA (1–100μM, dependent on mutant) versus a high or maximal concentration of GABA (10mM-600mM, dependent on mutant). We then calculated GABA EC_{50} for each mutant (with previously measured Hill coefficients and the low/high GABA current ratios determined) using the standard Hill equation:

$$\theta=[\mathrm{GABA}_{\mathrm{low}}]^{\mathrm{nH}}/(\mathrm{EC}_{50}{}^{\mathrm{nH}}+[\mathrm{GABA}_{\mathrm{low}}]^{\mathrm{nH}}),$$

where nH is the Hill coefficient, $GABA_{low}$ is the low test concentration of GABA, and θ is the ratio of current response to a low concentration of GABA versus a high or maximal concentration of GABA.

Flurazepam and pentobarbital potentiation, DMCM inhibition, or flumazenil (Ro15–1788) antagonism of BZD-potentiation of IGABA were recorded at GABA EC_{15}. Modulation of GABA current is reported in fold-changes, defined as $I_{GABA+DRUG(s)}/I_{GABA}$, where $I_{GABA+DRUG(s)}$ is the current response in the presence of the drug(s) tested, and I_{GABA} is the control GABA-induced current. Maximal potentiation of I_{GABA} was measured with 10μm flurazepam or 25–50μM pentobarbital. Maximal inhibition of I_{GABA} was measured with 100μM or 1μM DMCM. Flumazenil antagonism of BZD-induced modulation of I_{GABA} was measured by co-applying 1μM flumazenil with 10μm flurazepam or 1μM DMCM.

2.4. Rate of MTS modification

We previously established that all of the introduced cysteines were accessible to MTS modification (Boileau et al., 1999; Boileau et al., 2002; Holden and Czajkowski, 2002; Kloda and Czajkowski, 2007; Newell et al., 2004; Wagner and Czajkowski, 2001). GABA current (I_{GABA}) for each oocyte was stabilized before addition of MTS reagents by applying successive pulses of GABA, separated by 2min washes, until I_{GABA} varied by <5% to ensure that the observed changes in I_{GABA} after MTS application were due to MTS modification of the introduced cysteine. The rate of MTS covalent modification of the introduced cysteines in the absence of drug was determined by measuring the outcome of sequential applications of MTS reagents on I_{GABA}. The protocol was as follows: A concentration of $EC_{20–30}$ GABA (for MTS potentiation of I_{GABA}) or $EC_{50–65}$ (for MTS inhibition of I_{GABA})was applied for 5 sec; the cell was washed for 1min 40sec-1min 53sec; MTS reagent was applied for 7–20 sec; the cell was washed for 1 min; and the procedure was repeated until I_{GABA} no longer changed indicating that the reaction reached completion. Time and concentration of MTS application for each mutant was chosen such that at least six I_{GABA} measurements were obtained before the reaction reached completion, where most importantly the rise/decay phase of the exponential curve was defined by at least 3 data points. As such, concentrations of MTS reagent and time of application at each cysteine varied as follows: α_1T60C-500μM MTSEA-biotin, 10 sec; α_1S68C-100μM MTSES, 7 sec; α_1E122C-1μM MTSEA-biotin, 10 sec; α_1R131C-100μM MTSEA-biotin, 10 sec; β_2L99C-300μM MTSEA-biotin, 10 sec; β_2T160C-200nM MTSEA-biotin, 10 sec; β_2G203C-400nM MTSEA-biotin, 10 sec; β_2P206C-200μM MTSEA-biotin, 10 sec; β_2R207C-200μM MTSEA-biotin, 10 sec; β_2S209C-200μM MTSEA-biotin, 20 sec.

The effects of modulators on the rates of MTS modification were tested by co-applying 10μM flurazepam, 100nM-1μM DMCM, flumazenil (1μM or 25–50μM pentobarbital with MTSEA-biotin, with the exception of α_1S68C, in which case they were co-applied with MTSES. Pentobarbital concentrations used in rate experiments were chosen such that they did not elicit more than 5% of maximal I_{GABA} (i.e., were not activating). DMCM concentrations were chosen based on the effectiveness of DMCM-induced I_{GABA} inhibition and wash-out. Thus, the lower concentration of DMCM (100nM), used in rate experiments at α_1E122C$\beta_2\gamma_2$ and α_1P206C$\beta_2\gamma_2$ receptors, was saturating and significantly inhibited I_{GABA} (0.45-fold) but more effectively washed-out relative to 1μM DMCM. For these studies, I_{GABA} was stabilized before MTS application as follows: A fixed concentration of EC_{20}-EC_{65} GABA was applied for 5 sec; the cell was washed for 1min 40 sec-1min 53 sec; flurazepam, DMCM, flumazenil, or pentobarbital was applied for 7–20 sec; the cell was washed for 1–5 min; and the procedure was repeated until I_{GABA} was stabilized (e.g. I_{GABA} varied <5%). This procedure was subsequently repeated for MTS rate measurements while successively co-applying MTS with drug until the reaction reached completion (i.e. no additional change in I_{GABA}). For each mutant, application times were kept constant between

control (MTS alone) and experimental (MTS+drug) conditions, while MTS concentrations were varied as necessary. At least two different concentrations of MTS were used for rate measurements, to verify that the rates were independent of the MTS-reagent concentration. In all cases, the second order rate constants were independent of the reagent concentrations.

For all rate experiments, the change in I_{GABA} (decrease or increase) after each reagent application was plotted versus cumulative time of MTS exposure. The change in I_{GABA} (ΔI_{GABA}) at each time-point was defined as: $\Delta I_{GABA} = (I_{GABA}/I_{GABAo}) - 1$, where I_{GABA} is the peak GABA current measured after each successive MTS application and I_{GABAo} refers to peak stabilized GABA current prior to MTS application at time 0. The ΔI_{GABA} versus cumulative time of MTS exposure was fit with a single-exponential association or decay function: y= span × e^{-kt} + plateau, where *k* is the pseudo-first-order rate constant of the reaction (Prism, GraphPad Software Inc., San Diego, CA). Plateau is the ΔI_{GABA} at the end of the reaction when I_{GABA} is no longer changing and is defined by the curve fit. Because ΔI_{GABA} is defined relative to I_{GABA} at time zero (i.e. $\Delta I_{GABA} = (I_{GABA}/I_{GABAo}) - 1$), span=0-plateau. The second-order rate constants (k_2) were determined by dividing *k* by the concentration of MTS reagent used in the rate measurement (Pascual and Karlin, 1998) and are reported in Table 1. For easier visual comparisons between control and experimental data sets, the data in Figures 2, 3, and 4, were normalized to the maximum effect of the MTS reagent, where the ΔI_{GABA} at each time point was normalized to the plateau: [(I_{GABA}/I_{GABAo})-1]/plateau.

2.5. Statistical analysis

All data were from at least three different oocytes from at least two different frogs. Data from MTS modification experiments were fit using nonlinear regression analysis included in the Prism software package (GraphPad Software Inc., San Diego, CA). Significant differences in k_2 (second order rate) values were determined by one-way ANOVA, followed by a post hoc Dunnett's test (GraphPad Software Inc., San Diego, CA). We also used FDR (false discovery rate) analysis to examine statistical differences in MTS rates of reaction between control and experimental conditions at β_2P206C (Herrington, 2002).

3. Results

The aim of this study was to test the following distinct, yet related, hypotheses: (1) Allosteric modulators induce conformational movements in the GABA binding site interface, (2) Positive and negative BZD modulators induce distinct movements within the GABA binding site interface, which encode a BZD's efficacy, and (3) Positive allosteric modulators that bind to different sites on the GABAR initiate similar movements at the GABA binding site interface. To test these hypotheses, we introduced cysteine residues throughout the GABA binding site interface and measured their rates of modification by sulfhydryl specific reagents in the absence or presence of flurazepam (BZD-site positive modulator), DMCM (BZD-site negative modulator), flumazenil (BZD-site zero modulator) or pentobarbital (PB, barbiturate-site positive modulator). The rate of covalent modification depends on the local physical and electrostatic environment near the introduced cysteine. As such, any alteration in the modification rate of a cysteine in the presence of ligand is indicative of a change in the local environment of the cysteine and thus a ligand-induced conformational movement in the protein.

3.1. Expression and functional characterization of cysteine mutant receptors

The GABA binding site is comprised of six non-contiguous regions, arbitrarily designated loops A (β-strand 4), B (β-strand 7), and C (β-strand 10) on the β_2 subunit and loops D (β-strand 2), E (β-strand 5–6) and F (loop 9) on the α_1 subunit (Galzi and Changeux, 1995). We

individually mutated residues in Loop D (T60, S68) and loop E (E122, R131) of the α_1 subunit and, loop A (L99), loop B (T160) and loop C (S209, R207, P206 and G203) of the β_2 subunit to cysteine (Fig. 1). Mutant α_1 and β_2 subunits were co-expressed with WT α_1 or β_2 subunits and the γ_2 subunit in *Xenopus laevis* oocytes to form $\alpha_1\beta_2\gamma_2$ GABARs, which were then analyzed using two-electrode voltage clamp. All of the mutant subunits formed functional channels ($I_{GABAmax}$ = 1–20μA). Previously, we determined the GABA EC_{50} values for these mutant receptors (Boileau et al., 1999; Boileau et al., 2002; Holden and Czajkowski, 2002; Kloda and Czajkowski, 2007; Newell et al., 2004; Wagner and Czajkowski, 2001). In this study, we estimated the GABA EC_{50} of each oocyte we recorded from by measuring the ratio of the amplitude of current induced by a low versus maximal concentration of GABA (see **Materials and Methods**). Our GABA EC_{50} estimates replicated our data previously reported, where β_2 mutants T160C, G203C, R207C, S209C and α_1 mutants S68C, E122C, R131C significantly increased GABA EC_{50} values 12-, 2700-, 29-, 5-, 6-, 3-, and 23-fold relative to WT (WT EC_{50}= 10.7 +/− 1.3 μM, n = 6), respectively. Cysteine substitution of α_1T60, β_2L99 and β_2P206 had no significant effect on GABA EC_{50} compared to WT receptors.

The mutant receptors were all responsive to BZD and pentobarbital (PB) modulation of I_{GABA}. Flurazepam maximally potentiated GABA ($EC_{10–15}$) currents in mutant receptors 2.2 to 3.3-fold, comparable to WT receptors (WT potentiation = 2.6; (Boileau and Czajkowski, 1999; Hanson and Czajkowski, 2008)). DMCM maximally attenuated GABA ($EC_{10–15}$) current in mutant receptors 0.27 to 0.65-fold, similar to WT GABARs (0.62-fold; (Boileau and Czajkowski, 1999; Hanson and Czajkowski, 2008)). The BZD antagonist flumazenil had no effect on GABA-gated current in mutant receptors tested (α_1E122C$\beta_2\gamma_2$ and α_1R131C$\beta_2\gamma_2$) and attenuated the potentiating and inhibiting actions of flurazepam and DMCM respectively, as expected for a BZD-site antagonist. Low, modulating concentrations (25–50μM) of PB, potentiated GABA ($EC_{10–15}$) current from mutant receptors between 3 and 6-fold, comparable to its effects on WT receptors.

3.2 Effects of flurazepam, DMCM, Flumazenil, and PB on rates of modification of introduced cysteines in the GABAR α_1 subunit

Previously, we demonstrated that flurazepam altered the rate of modification of α_1E122C and α_1R131C (Kloda and Czajkowski, 2007). α_1E122 and α_1R131 are located on β-strands 5 and 6 (loop E), respectively, at the GABA binding interface (Fig 1). Here, we examined and compared the effects of DMCM, flurazepam, flumazenil and PB on the rate of modification of these residues. Flurazepam, DMCM and PB each significantly slowed MTSEA-biotin modification of α_1E122C (Fig. 2; Fig. 5; Table 1), suggesting that this residue and/or residues in close proximity undergo conformational rearrangement in the presence of these allosteric modulators. Despite the fact that flurazepam is a positive modulator and DMCM is a negative modulator, both induced a similar 1.7-fold reduction ($p<0.05$) in the rate of reaction of MTSEA-biotin at α_1E122C (Table 1; Fig. 5A). At α_1R131C$\beta_2\gamma_2$ receptors, MTSEA-biotin reacted 2.1- and 1.9-fold faster in the presence of BZD-site ligands flurazepam and DMCM, respectively ($p<0.01$; Fig. 2; Fig. 5A; Table 1). Interestingly, unlike flurazepam and DMCM, flumazenil (BZD-site antagonist) did not significantly alter the rate of modification at α_1R131C (k_2 = 307±4.3 $M^{-1}s^{-1}$; n=3) or α_1E122C (k_2 = 31,430±3617 $M^{-1}s^{-1}$; n=4) indicating that simple occupation of the BZD site is not sufficient to induce structural rearrangements at the GABA binding interface. Low, non-activating concentrations of PB significantly slowed MTSEA-biotin modification of α_1E122C 1.5-fold (Fig. 2; Fig. 5A; Table 1) but had no effect on the rate of modification of α_1R131C indicating that conformational movements induced by PB and BZDs are distinct.

Two additional α_1 subunit cysteine mutations (T60C, S68C), located on either end of β-strand 2 (loop D), were also examined (Fig 1). Based on comparisons between the agonist

bound crystal structure of the AChBP (acetylcholine binding protein) and the 4Å resolved cryo-EM structure of the nicotinic acetylcholine receptor (Unwin, 2005), as well as crystal structures of bacterial LGIC (ligand-gated ion channel) homologues, ELIC and GLIC, in presumed closed and open channel conformations (see (Corringer et al., 2010) for review), it has been postulated that the β-strands in the extracellular domain rotate upon agonist-mediated channel activation. If BZD binding initiates similar movements in the GABAR as agonist-mediated activation of structurally related pentameric LGICs, we might expect residues in β-strand 2 (loop D), as well as those in β-strands 5 and 6 (loop E), to undergo structural rearrangements upon binding of BZDs. Unlike residues on β-strands 5 and 6 (α_1R131C and α_1E122C), the rates of MTS modification of α_1S68C and α_1T60C were not significantly altered in the presence of flurazepam or DMCM ($p>0.05$; Fig. 3;Fig 5A;Table 1) suggesting that BZD binding does not induce a concerted movement of the inner β-strands of the α_1 subunit. We cannot, however, rule out the possibility that BZD-induced movements occurred but were not detected by our experimental approach. Low modulatory concentrations of PB significantly accelerated the rate of MTSES modification of α_1S68C ($p<0.05$; Fig. 3;Fig. 5A;Table 1), consistent with our previous data that showed that this residue undergoes a change in environment in the presence of PB when expressed in the background of $\alpha_1\beta_2$ receptors (Holden and Czajkowski, 2002). Since the rate of modification of α_1S68C was altered in the presence of PB but not flurazepam or DMCM, the data provide additional evidence that the binding of PB and BZDs induce distinct movements at the GABA binding site interface.

3.3. Effects of flurazepam, DMCM, and PB on the rate of modification of cysteine substitutions in the β_2 subunit

We were particularly interested in examining the rate of modification of cysteine mutations in loop C (β-strand 10) of the β_2 subunit, as loop C is postulated to be a key region involved in agonist-mediated receptor activation in members of the cys-loop LGIC super family (see (Sine and Engel, 2006) for review). Upon agonist binding, Loop C is proposed to cap the site and trap the agonist, which then triggers a series of down-stream conformational events that ultimately leading to channel opening (Celie et al., 2004; Gao et al., 2005; Law et al., 2005; Lee and Sine, 2005; Unwin, 2005; Wang et al., 2009). If binding of positive allosteric modulators triggers some of the same conformational movements at the orthosteric site that are induced by agonist binding, we might expect to detect structural rearrangements in loop C upon binding of flurazepam and potentiating concentrations of PB. Due to its speculated role in coupling agonist binding to channel gating (Boileau et al, 2002), we also examined residue β_2L99C in Loop A (β-strand 4). Moreover, we examined β_2T160C in loop B (β-strand 7), since previous work had shown that this region undergoes structural rearrangement in the presence of GABA and modulatory concentrations of PB (Newell et al, 2004).

Flurazepam, DMCM and PB had no significant effects on the rates of MTSEA-biotin modification of β_2L99C (Loop A), β_2T160C (Loop B), β_2G203C, β_2R207C, or β_2S209C (loop C) (Fig. 4B; Fig. 5B; Table 1). MTSEA-biotin reacted significantly faster at β_2P206C (1.9-fold) in the presence of PB ($p<0.01$; Fig. 4A; Fig. 5B; Table 1). In the presence of flurazepam and DMCM, the rates of MTSEA-biotin reaction at β_2P206C were increased 1.6-fold (Table 1, Fig. 5B), but the data did not reach statistical significance using an ANOVA. False discovery rate analysis of the data (FDR; Herrington, 2002), however, suggested that flurazepam and DMCM significantly increased MTSEA-biotin reaction rates.

4. Discussion

4.1. BZD agonist and inverse agonist actions induce structural rearrangement at the GABA binding site interface

Both a BZD-site agonist and a BZD-site inverse agonist changed the rate of modification of two residues in Loop E of the GABAR α_1 subunit, α_1E122C (on β-strand 5) and α_1R131C (on β-strand 6) (Fig. 2; Fig 5A; Table 1). The data demonstrate that BZDs induce a conformational movement near these residues and that structural changes initiated at the α/ γ subunit BZD binding site interface can extend over considerable distance. In the α_1 subunit, β-strands 5 and 6 (Loop E of the GABA binding site) are connected to the BZD-binding pocket (Loop A) by a six-residue linker element (Fig. 1). We envision that BZD-induced conformational movements at the α/γ BZD binding site interface are propagated across the α_1 subunit via this linker to the β/α GABA binding site interface. Consistent with this idea, it has been proposed that Zn^{2+} binding to this linker region in the structurally related glycine receptor mediates Zn^{2+}-mediated allosteric inhibition of glycine receptor function by hindering agonist-induced movement at the adjacent glycine binding site interfaces (Miller et al., 2008).

Flurazepam (BZD site agonist) and DMCM (BZD site inverse agonist) both induced nearly identical changes in the rates of modification of α_1E122C and α_1R131C (Fig. 5; Table 1), suggesting that the movements being detected near these residues are similar and are associated with BZD binding site occupation and do not reflect whether a BZD is a positive or negative modulator. Alternatively, it is possible flurazepam and DMCM trigger structurally distinct movements that are not detectable by our experimental approach. For example, if flurazepam and DMCM initiate different movements such that the resulting physico/chemical environments around the introduced cysteines were coincidentally nearly identical, then the change in the rate of modification in the presence of either BZD-ligand would be similar. To help distinguish between these possibilities, we measured the rate of modification of only those cysteine substitutions conformationally sensitive to modulatory BZDs, α_1E122C and α_1R131C, in the presence of the BZD-site antagonist flumazenil. We reasoned that if the movements induced by flurazepam and DMCM carry no information regarding efficacy, a BZD-site antagonist (zero modulator) would alter the rate of modification of α_1E122C and α_1R131C to the same extent as flurazepam and DMCM. However, flumazenil did not alter the rate of modification of α_1R131C or α_1E122C. This finding indicates the movements induced by flurazepam and DMCM do not simply reflect BZD binding site occupation, but instead correlate with the ability of these BZD-site ligands to modulate GABAR function (efficacy). Further studies will be necessary, using different experimental approaches (e.g. voltage clamp fluorimetry) and multiple BZD-site ligands with different structures and efficacies, to distinguish the specific movements induced by these modulators. Nonetheless, while our methodological approach cannot distinguish whether a BZD-site ligand is a positive versus negative modulator, the data demonstrate that BZD efficacy is, at least in part, encoded at the GABA binding site interface. Although the temporal resolution of these conformational movements initiated by BZDs has yet to be determined, we hypothesize that BZD-induced structural perturbations at the GABA binding interface trigger structural movements at or near the transmembrane domains, which ultimately alter GABAR gating machinery. In support of our hypothesis, previous studies have shown that BZDs induce structural rearrangements in the α_1 M3 transmembrane helix of the receptor (Williams and Akabas, 2000) and in γ_2 Loop F(9) near the transmembrane region (Hanson and Czajkowski, 2008).

Surprisingly, flurazepam and DMCM did not significantly alter the rates of modification of the majority of introduced cysteines in the β_2 subunit, suggesting that BZD-induced conformational movements at the α/γ BZD binding site interface do not extend to these

regions on the β_2 subunit. However, we cannot rule out the possibility that BZD-induced movements may have occurred such that the physico-chemical environment surrounding the cysteines was unchanged, thus rendering these movements undetectable using the substituted cysteine accessibility method. While not statistically significant using an ANOVA analysis, flurazepam and DMCM each increased the rate of modification of β_2P206C 1.6-fold (Fig. 4A; Fig. 5; Table 1), which when analyzed using a less stringent FDR analysis were significant, hinting that BZDs may induce movements at or near this residue. We previously demonstrated that GABA significantly increased the rate of modification at β_2P206C by 2.6-fold (Wagner and Czajkowski, 2001) indicating that GABA binding and/or GABA-mediated channel activation triggers structural rearrangements at or near this residue. We speculate that BZD-induced movements may not be as large or as wide spread as those induced by GABA since BZD binding in the absence of GABA does not under normal conditions gate the GABAR channel. Consistent with this idea, GABA induced a 3-fold decrease in the rate of modification of α_1E122C (Kloda and Czajkowski, 2007), while flurazepam and DMCM induced a more modest 1.7-fold decrease in rate (Table 1). Moreover, diazepam similarly induced a more limited conformational change in the α_1 M3 transmembrane helix relative to GABA (Williams and Akabas, 2000).

4.2. Flurazepam and PB induce different structural rearrangements at the GABA binding site interface

BZD-site ligands and low potentiating concentrations of PB had different effects on the rates of modification of α_1S68C and α_1R131C. At α_1S68C, flurazepam and DMCM had no effect on its modification rate, while PB significantly increased its rate of modification (Fig. 3B; Fig 5; Table 1). At α_1R131C, BZD-site ligands increased the modification rate, while PB had no effect (Fig 2C&D; Fig 5; Table 1). Furthermore, at Loop C residue β_2P206C, a larger increase in the rate of reaction in the presence of PB relative to flurazepam was observed. These results demonstrate that PB and flurazepam induce different structural rearrangements at or near these residues, indicating that the structural mechanisms underlying positive allosteric modulation by the general anesthetic PB is different than the mechanisms underlying BZD positive modulation. This divergence in structural mechanisms is consistent with the differential effects these drugs have on GABAR activation and single channel kinetics. The fact that PB can act as an agonist, while flurazepam cannot, may explain the differential effects of PB and flurazepam in loop C (β-strand 10), as closure or movement of loop C is associated with channel activation (see (Sine and Engel, 2006) for review). Additionally, general anesthetics such as PB and propofol increase channel open time durations whereas BZD-site positive modulators increase the frequency of channel opening (MacDonald et al., 1989;Mellor and Randall, 1997;Rogers et al., 1994;Steinbach and Akk, 2001;Twyman et al., 1989). Given that PB and BZDs bind to distinct sites on the GABAR (Amin, 1999;Belelli et al, 1999;Serafini et al, 2000), one might predict that the receptor would undergo different structural rearrangements upon binding of each drug. Our findings provide experimental evidence for this idea. Additional supporting evidence comes from studies that demonstrate propofol and BZDs initiate different structural rearrangements in the GABAR α_1 M3 transmembrane helix (Williams and Akabas, 2000,2002). Taken together, the data suggest that the allosteric pathways governing positive modulation of the GABAR by different classes of modulators are distinct. Mapping these structural pathways is an important goal for future studies.

Abbreviations

BZD	benzodiazepine
GABAR	GABA-A receptor

MTSEA-Biotin	N-biotinaminoethyl methanethiosulfonate
MTSES	2-sulfonatoethyl methanethiosulfonate
DMCM	3-carbomethoxy-4-ethyl-6, 7-dimethoxy-β-carboline
Ro15–1788	flumazenil
PB	pentobarbital
LGIC	ligand-gated ion channel
AChBP	acetylcholine binding protein
GLIC	bacterial *Gloeobacter violaceus* pentameric LGIC homologue
ELIC	bacterial *Erwinia chrysanthemi* LGIC homologue

References

Amin J. A single hydrophobic residue confers barbiturate sensitivity to gamma-aminobutyric acid type C receptor. Mol Pharmacol 1999;55:411–423. [PubMed: 10051524]

Belelli I, Pistis I, Peters JA, Lambert JJ. General anaesthetic action at transmitter- gated inhibitory amino acid receptors. Trends Pharmacol Sci 1999;20:496–502. [PubMed: 10603492]

Boileau AJ, Czajkowski C. Identification of transduction elements for benzodiazepine modulation of the GABA(A) receptor: three residues are required for allosteric coupling. J Neurosci 1999;19:10213–10220. [PubMed: 10575018]

Boileau AJ, Evers AR, Davis AF, Czajkowski C. Mapping the agonist binding site of the GABAA receptor: evidence for a beta-strand. J Neurosci 1999;19:4847–4854. [PubMed: 10366619]

Boileau AJ, Kucken AM, Evers AR, Czajkowski C. Molecular dissection of benzodiazepine binding and allosteric coupling using chimeric gamma-aminobutyric acidA receptor subunits. Mol Pharmacol 1998;53:295–303. [PubMed: 9463488]

Boileau AJ, Newell JG, Czajkowski C. GABA(A) receptor beta 2 Tyr97 and Leu99 line the GABA-binding site. Insights into mechanisms of agonist and antagonist actions. J Biol Chem 2002;277:2931–2937. [PubMed: 11711541]

Campo-Soria C, Chang Y, Weiss DS. Mechanism of action of benzodiazepines on GABAA receptors. Br J Pharmacol 2006;148:984–990. [PubMed: 16783415]

Celie PH, van Rossum-Fikkert SE, van Dijk WJ, Brejc K, Smit AB, Sixma TK. Nicotine and carbamylcholine binding to nicotinic acetylcholine receptors as studied in AChBP crystal structures. Neuron 2004;41:907–914. [PubMed: 15046723]

Corringer PJ, Baaden M, Bocquet N, Delarue M, Dufresne V, Nury H, Prevost M, Van Renterghem C. Atomic structure and dynamics of pentameric ligand-gated ion channels: new insight from bacterial homologues. J Physiol 2010;588:565–572. [PubMed: 19995852]

Downing SS, Lee YT, Farb DH, Gibbs TT. Benzodiazepine modulation of partial agonist efficacy and spontaneously active GABA(A) receptors supports an allosteric model of modulation. Br J Pharmacol 2005;145:894–906. [PubMed: 15912137]

Galzi JL, Changeux JP. Neuronal nicotinic receptors: molecular organization and regulations. Neuropharmacology 1995;34:563–582. [PubMed: 7566492]

Gao F, Bren N, Burghardt TP, Hansen S, Henchman RH, Taylor P, McCammon JA, Sine SM. Agonist-mediated conformational changes in acetylcholine-binding protein revealed by simulation and intrinsic tryptophan fluorescence. J Biol Chem 2005;280:8443–8451. [PubMed: 15591050]

Goldschen-Ohm MP, Wagner DA, Petrou S, Jones MV. An epilepsy-related region in the GABA(A) receptor mediates long-distance effects on GABA and benzodiazepine binding sites. Mol Pharmacol 2010;77:35–45. [PubMed: 19846749]

Hanson SM, Czajkowski C. Structural mechanisms underlying benzodiazepine modulation of the GABA(A) receptor. J Neurosci 2008;28:3490–3499. [PubMed: 18367615]

Hemmings HC Jr, Akabas MH, Goldstein PA, Trudell JR, Orser BA, Harrison NL. Emerging molecular mechanisms of general anesthetic action. Trends Pharmacol Sci 2005;26:503–510. [PubMed: 16126282]

Holden JH, Czajkowski C. Different residues in the GABA(A) receptor alpha 1T60- alpha 1K70 region mediate GABA and SR-95531 actions. J Biol Chem 2002;277:18785–18792. [PubMed: 11896052]

Jones-Davis DM, Song L, Gallagher MJ, Macdonald RL. Structural determinants of benzodiazepine allosteric regulation of GABA(A) receptor currents. J Neurosci 2005;25:8056–8065. [PubMed: 16135763]

Kloda JH, Czajkowski C. Agonist-, antagonist-, and benzodiazepine-induced structural changes in the alpha1 Met113-Leu132 region of the GABAA receptor. Mol Pharmacol 2007;71:483–493. [PubMed: 17108261]

Kucken AM, Wagner DA, Ward PR, Teissére JA, Boileau AJ, Czajkowski C. Identification of benzodiazepine binding site residues in the [gamma]2 subunit of the gamma-aminobutyric acid(A) receptor. Mol Pharmacol 2000;57:932–939. [PubMed: 10779376]

Lavoie AM, Twyman RE. Direct evidence for diazepam modulation of GABAA receptor microscopic affinity. Neuropharmacology 1996;35:1383–1392. [PubMed: 9014155]

Law RJ, Henchman RH, McCammon JA. A gating mechanism proposed from a simulation of a human alpha7 nicotinic acetylcholine receptor. Proc Natl Acad Sci U S A 2005;102:6813–6818. [PubMed: 15857954]

Lee WY, Sine SM. Principal pathway coupling agonist binding to channel gating in nicotinic receptors. Nature 2005;438:243–247. [PubMed: 16281039]

Liman ER, Tytgat J, Hess P. Subunit stoichiometry of a mammalian K+ channel determined by construction of multimeric cDNAs. Neuron 1992;9:861–871. [PubMed: 1419000]

MacDonald RL, Rogers CJ, Twyman RE. Barbiturate regulation of kinetic properties of the GABAA receptor channel of mouse spinal neurones in culture. J Physiol (Lond) 1989;417:483–500. [PubMed: 2482885]

Mellor JR, Randall AD. Frequency-dependent actions of benzodiazepines on GABAA receptors in cultured murine cerebellar granule cells. J Physiol 1997;503 (Pt 2):353–369. [PubMed: 9306278]

Miller PS, Topf M, Smart TG. Mapping a molecular link between allosteric inhibition and activation of the glycine receptor. Nat Struct Mol Biol 2008;15:1084–1093. [PubMed: 18806798]

Mitchell EA, Herd MB, Gunn BG, Lambert JJ, Belelli D. Neurosteroid modulation of GABAA receptors: molecular determinants and significance in health and disease. Neurochem Int 2008;52:588–595. [PubMed: 18055067]

Newell JG, McDevitt RA, Czajkowski C. Mutation of glutamate 155 of the GABAA receptor beta2 subunit produces a spontaneously open channel: a trigger for channel activation. J Neurosci 2004;24:11226–11235. [PubMed: 15601928]

Padgett CL, Lummis SC. The F-loop of the GABA A receptor gamma2 subunit contributes to benzodiazepine modulation. J Biol Chem 2008;283:2702–2708. [PubMed: 17974564]

Pascual JM, Karlin A. State-dependent accessibility and electrostatic potential in the channel of the acetylcholine receptor. Inferences from rates of reaction of thiosulfonates with substituted cysteines in the M2 segment of the alpha subunit. J Gen Physiol 1998;111:717–739. [PubMed: 9607933]

Pritchett DB, Sontheimer H, Shivers BD, Ymer S, Kettenmann H, Schofield PR, Seeburg PH. Importance of a novel GABAA receptor subunit for benzodiazepine pharmacology. Nature 1989;338:582–585. [PubMed: 2538761]

Robertson GA, Warmke JM, Ganetzky B. Potassium currents expressed from Drosophila and mouse eag cDNAs in Xenopus oocytes. Neuropharmacology 1996;35:841–850. [PubMed: 8938715]

Rogers CJ, Twyman RE, Macdonald RL. Benzodiazepine and beta-carboline regulation of single GABAA receptor channels of mouse spinal neurones in culture. J Physiol (Lond) 1994;475:69–82. [PubMed: 7514665]

Rusch D, Forman SA. Classic benzodiazepines modulate the open-close equilibrium in alpha1beta2gamma2L gamma-aminobutyric acid type A receptors. Anesthesiology 2005;102:783–792. [PubMed: 15791108]

Serafini R, Bracamontes J, Steinbach JH. Structural domains of the human GABAA receptor beta3 subunit involved in the actions of pentobarbital. J Physiol 2000;524(Pt 3):649– 676. [PubMed: 10790149]

Sigel E. Mapping of the Benzodiazepine Recognition Site on GABA(A) Receptors. Curr Top Med Chem 2002;2:833–839. [PubMed: 12171574]

Sine SM, Engel AG. Recent advances in Cys-loop receptor structure and function. Nature 2006;440:448–455. [PubMed: 16554804]

Smith GB, Olsen RW. Functional domains of GABAA receptors. Trends Pharmacol Sci 1995;16:162–168. [PubMed: 7624971]

Steinbach JH, Akk G. Modulation of GABA(A) receptor channel gating by pentobarbital. J Physiol 2001;537:715–733. [PubMed: 11744750]

Thompson SA, Smith MZ, Wingrove PB, Whiting PJ, Wafford KA. Mutation at the putative GABA(A) ion-channel gate reveals changes in allosteric modulation. Br J Pharmacol 1999;127:1349–1358. [PubMed: 10455284]

Twyman RE, Rogers CJ, Macdonald RL. Differential regulation of gamma- aminobutyric acid receptor channels by diazepam and phenobarbital. Ann Neurol 1989;25:213–220. [PubMed: 2471436]

Unwin N. Refined structure of the nicotinic acetylcholine receptor at 4A resolution. J Mol Biol 2005;346:967–989. [PubMed: 15701510]

Wagner DA, Czajkowski C. Structure and dynamics of the GABA binding pocket: A narrowing cleft that constricts during activation. J Neurosci 2001;21:67–74. [PubMed: 11150321]

Wang HL, Toghraee R, Papke D, Cheng XL, McCammon JA, Ravaioli U, Sine SM. Single-channel current through nicotinic receptor produced by closure of binding site C-loop. Biophys J 2009;96:3582–3590. [PubMed: 19413963]

Williams DB, Akabas MH. Benzodiazepines induce a conformational change in the region of the gamma-aminobutyric acid type A receptor alpha(1)-subunit M3 membrane- spanning segment. Mol Pharmacol 2000;58:1129–1136. [PubMed: 11040062]

Williams DB, Akabas MH. Structural evidence that propofol stabilizes different GABA(A) receptor states at potentiating and activating concentrations. J Neurosci 2002;22:7417–7424. [PubMed: 12196563]

Web References

Herrington, R. Controlling the False Discovery Rate in Multiple Hypothesis Testing. 2002. http://www.unt.edu/benchmarks/archives/2002/april02/rss.htm

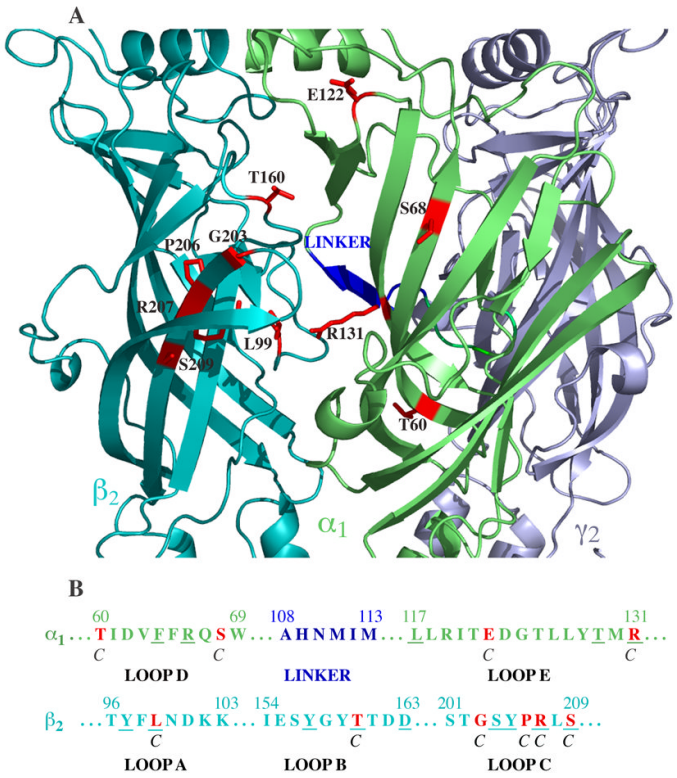

Figure 1. Location of residues substituted to cysteine at the GABA binding interface of the GABAR

(A) Homology model of the α_1 (cyan), β_2 (green) and γ_2 (light grey) subunits of the GABAR with residues substituted to cysteine labeled and highlighted in red. The region in the α_1 subunit that links the BZD and GABA binding interfaces (denoted LINKER) is highlighted in dark blue. (B) Partial sequences of α_1 (cyan) and β_2 (green) GABA binding site loop regions A (β-strand 4), B (β-strand 7), C (β-strand 10), D (β-strand 2), and E (β-strand 5–6), with residues substituted to cysteine in red (and denoted with the letter C below the residue). Numbering is based on mature protein sequences. LINKER residues are in dark blue, and residues previously implicated in lining the GABA binding pocket are underlined.

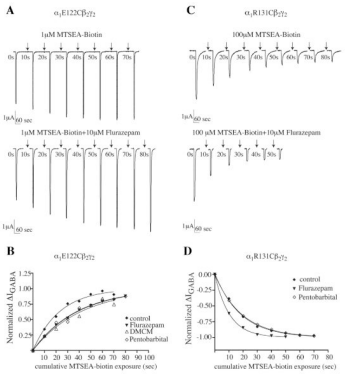

Figure 2. Effects of allosteric modulators on the rate of MTSEA-Biotin modification of α_1 subunit cysteine substitutions in loop E

(A) Representative GABA evoked (~$EC_{20–30}$) currents following successive 10 second MTSEA-biotin applications (arrows) in the absence (top traces) and presence (bottom traces) of 10μM flurazepam at $\alpha_1E122C\beta_2\gamma_2$ receptors. (B) Representative rates of reaction of MTSEA-biotin in the absence or presence of 10μM flurazepam, 100nM DMCM, or 50μM pentobarbital at $\alpha_1E122\beta_2\gamma_2$mutant receptors. Allosteric modulators significantly slowed the rate of reaction at position 122. (C) Representative GABA-evoked (~EC_{50}) currents following successive MTSEA-biotin applications (arrows) in the absence (top traces) and presence (bottom traces) of 10μM flurazepam at $\alpha_1R131C\beta_2\gamma_2$ receptors. (D) Representative rates of reaction of MTSEA-biotin in the absence and presence of 10μM flurazepam or 25μM pentobarbital at $\alpha_1R131C\beta_2\gamma_2$ receptors. Rate experiments were preformed as described under Materials and Methods. Increases or decreases in I_{GABA} (panels B & D) were plotted versus cumulative time of MTS exposure. Data were normalized and fit to a single-phase exponential decay as described in Materials and Methods. As multiple concentrations of MTS were used for the rate experiments, only representative rate plots, all obtained using the same concentration of MTS reagent, are shown for graphical clarity and comparative accuracy. For comparison of averaged normalized rates, see Figure 5.Se cond-order rate constants for MTS modification of α_1 subunit cysteine substitutions are summarized in TABLE 1.

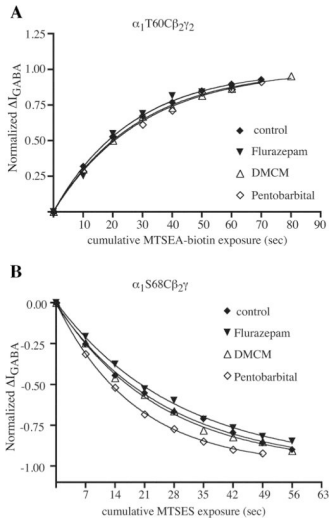

Figure 3. Effects of allosteric modulators on the rate of MTS modification of α_1 subunit cysteine substitutions in loop D

(A) Representative rates of reaction of MTSES in the absence and presence of 10μM flurazepam, 1μM DMCM, or 50μM pentobarbital at α_1S68C$\beta_2\gamma_2$ mutant receptors. (B) Representative rates of reaction of MTSEA-biotin in the absence and presence of 10μM flurazepam, 1μM DMCM, and 50μM pentobarbital at α_1T60C$\beta_2\gamma_2$ mutant receptors. Allosteric modulation by pentobarbital, but not BZD-site ligands DMCM or flurazepam, significantly slowed the rate of MTS reaction at S68C. The rate of MTS reaction at T60C was not significantly altered in the presence of any allosteric modulator tested. Data were acquired, normalized, and fit to a single-phase exponential decay as described in Fig 2 and Materials and Methods. Second-order rate constants for MTS modification of α_1 subunit cysteine substitutions are summarized in TABLE 1.

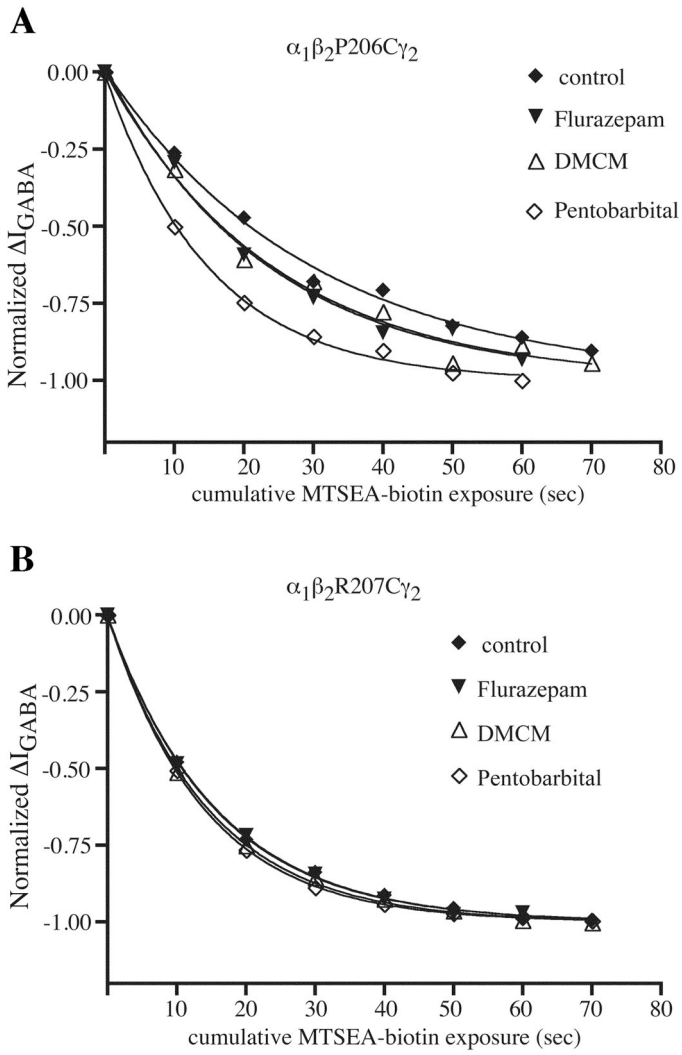

Figure 4. Effects of allosteric modulators on the rate of MTSEA-biotin modification of β_2 subunit cysteine substitutions in loop C

(A) Representative rates of reaction of MTSEA-biotin in the absence and presence of 10μM flurazepam, 100nM DMCM, and 50μM pentobarbital at $\alpha_1\beta_2$P206Cγ_2 receptors. Of the loop C residues tested, only position 206 displayed altered rates of reaction in the presence of allosteric modulators. (B) Representative rates of reaction of MTSEA-biotin in the absence and presence of 10μM flurazepam, 1μM DMCM, and 25μM pentobarbital at $\alpha_1\beta_2$R207Cγ_2 receptors. Modulators had no effects on the rates of MTSEA-biotin modification at position 207. Data were acquired, normalized, and fit to a single-phase exponential decay as described in Fig 2 and Materials and Methods. Second-order rate constants for MTS modification of β_2 subunit cysteine substitutions are summarized in TABLE 1.

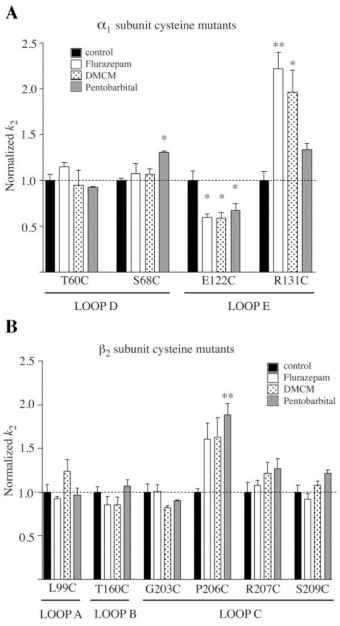

Figure 5. Summary of the effects of allosteric modulators on second-order rate constants (k_2) of MTS reaction at α_1 and β_2 subunit cysteine substitutions

Data were normalized to control second-order rate constants (the rate measured in the absence of allosteric modulators) and represent the mean±SEM of at least 3 experiments. Statistical significance was determined using a one-way ANOVA with Dunnett's post-test. (A) Rates of modification of cysteines on the α_1 subunit. Flurazepam and DMCM significantly slowed the rate of reaction at position α_1E122C (*$p<0.05$), while increasing the rate of reaction at position α_1R131C (**$p<0.01$). Pentobarbital, but not flurazepam or DMCM, significantly increased the rate of reaction at α_1S68C (*$p<0.05$). (B) Rates of modification of cysteines on the β_2 subunit. With the exception of β_2P206C, allosteric modulators did not alter the rate of reaction at any of the positions tested on the β_2 subunit. Modulatory pentobarbital significantly increased the rate of reaction at β_2P206C (**$p<0.01$) and, while not significant by ANOVA, false discovery rate analysis suggests that both flurazepam and DMCM speed the rate of reaction.

TABLE 1

Rates of MTS modification of cysteines introduced in the GABA binding site interface of the GABAR in the presence of BZD modulators Flurazepam and DMCM, and low concentrations of modulatory Pentobarbital

Rate of MTS reaction with introduced cysteines were measured, and second-order rate constants (k_2; $M^{-1}s^{-1}$) were calculated as described under **Materials and Methods** Second-order rate constants reflect the means±S.E.M

	Loop	Control		Flurazepam		DMCM		Pentobarbital	
Receptor		k_2	*n*	k_2	*n*	k_2	*n*	k_2	*n*
α_1T60Cβ_2 γ_2	D	74.4±5.2	4	85.5±3.3	5	70.6±12	3	68.8±0.73	3
α_1S68C$\beta_2\gamma_2$	D	407±8.1	4	432±44	3	429±23	3	526±4.7*	3
α_1R122C$\beta_2\gamma_2$	E	42703±4466	3	25.507±I730*	3	25,267±2392*	3	28,680±3396*	4
α_1R13lC$\beta_2\gamma_2$	E	455±49	3	953±78**	4	S45±100**	3	575±27	3
$\alpha_1\beta_2$L99Cγ_2	A	163±14	4	151±32	3	202±22	3	157±14	3
$\alpha_1\beta_2$T160Cγ_2	B	154525±9643	4	131570±15325	5	132456±12409	3	164800±12127	3
$\alpha_1\beta_2$G203Cγ_2	C	103.800±10018	3	103.967±8714	3	85138±2709	3	93.558±789	
$\alpha_1\beta_2$P206Cγ_2	C	159±6.4	4	255±29	5	260±35	5	300±20**	5
$\alpha_1\beta_2$R207Cγ_2	C	283±30	5	305±16	3	343±37	4	358±31	3
$\alpha_1\beta_2$S209Cγ_2	C	87.8±6.8	4	80.4±5.5	3	94.8±4.3	3	106.7±3.7	3

*Rates of reaction in the presence of ligand that were statistically significant from control, where $p < 0.5$.

**Rates of reaction in the presence of ligand that were statistically significant from control, where $p< 0.01$.